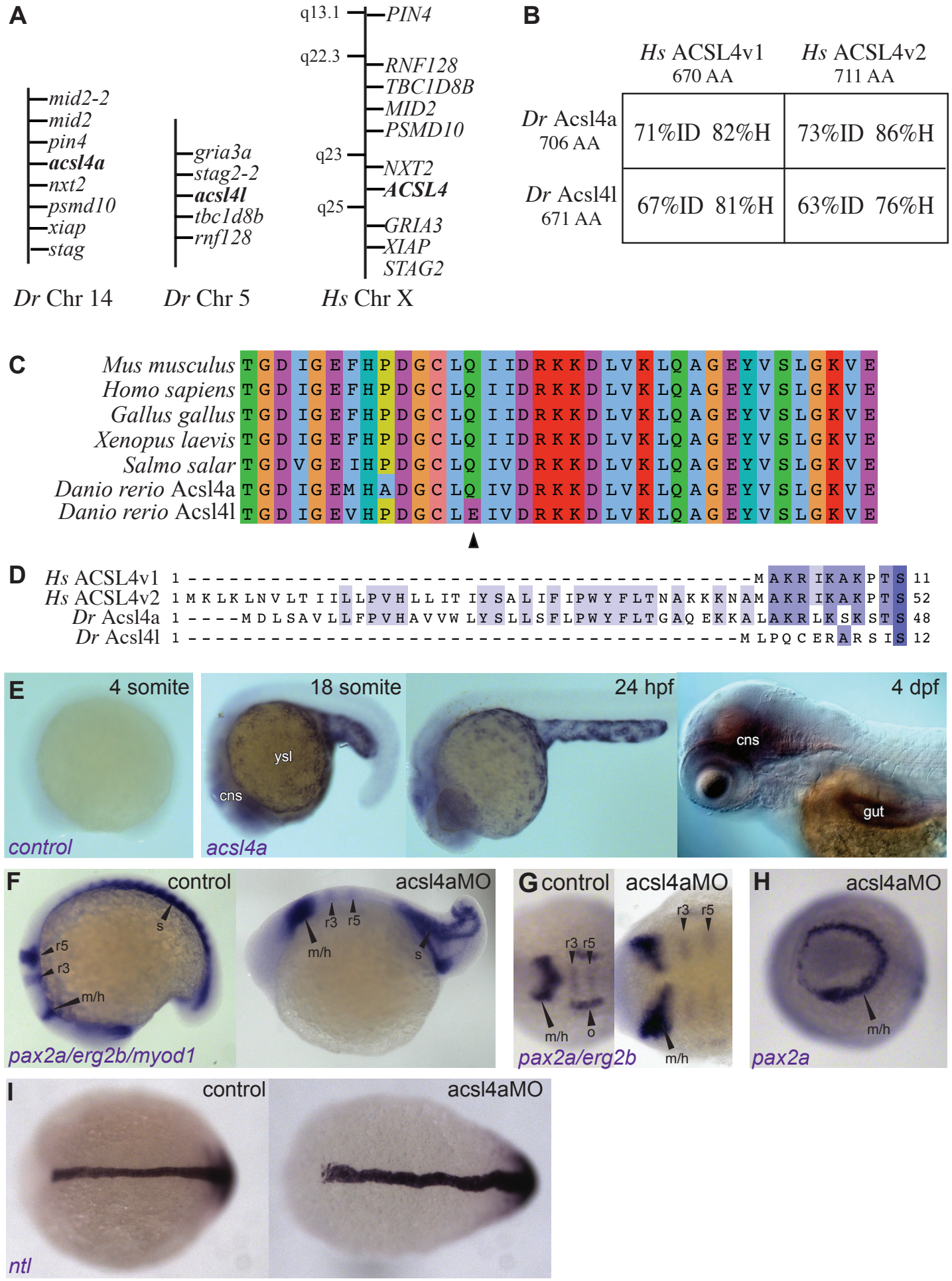
A
mid2-2
mid2
pin4
acsl4a
nxt2
psmd10
xiap
stag
Dr Chr 14
gria3a
stag2-2
acsl4l
tbc1d8b
rnf128
Dr Chr 5
q13.1
PIN4
q22.3
RNF128
TBC1D8B
MID2
PSMD10
q23
NXT2
ACSL4
q25
GRIA3
XIAP
STAG2
Hs Chr X
B
Hs ACSL4v1 670 AA
Hs ACSL4v2 711 AA
Dr Acsl4a 706 AA
71%ID 82%H
73%ID 86%H
Dr Acsl4l 671 AA
67%ID 81%H
63%ID 76%H
C
Mus musculus TGDIGEFHPDGCLQIIDRKKDLVKLQAGEYVSLGKVE
Homo sapiens TGDIGEFHPDGCLQIIDRKKDLVKLQAGEYVSLGKVE
Gallus gallus TGDIGEFHPDGCLQIIDRKKDLVKLQAGEYVSLGKVE
Xenopus laevis TGDIGEFHPDGCLQIIDRKKDLVKLQAGEYVSLGKVE
Salmo salar TGDVGEIHPDGCLQIVDRKKDLVKLQAGEYVSLGKVE
Danio rerio Acsl4a TGDIGEMHADGCLQIVDRKKDLVKLQAGEYVSLGKVE
Danio rerio Acsl4l TGDIGEVHPDGCLEIVDRKKDLVKLQAGEYVSLGKVE
D
Hs ACSL4v1 1 ----------MAKRIKAKPTS 11
Hs ACSL4v2 1 MKLKLNVLTIILLPVHLLITIYSALIFIPWYFLTNAKKKNAMAKRIKAKPTS 52
Dr Acsl4a 1 ----MDLSAVLLFPVHAVVWLYSLLSFLPWYFLTGAQEKKALAKRLKSKSTS 48
Dr Acsl4l 1 ----------MLPQCERARSIS 12
E
4 somite
control
18 somite
ysl
cns
acsl4a
24 hpf
4 dpf
cns
gut
F
control
acsl4aMO
s
r5
r3
m/h
r3
r5
m/h
s
pax2a/erg2b/myod1
G control
acsl4aMO
r3 r5
m/h
o
r3 r5
m/h
pax2a/erg2b
H
acsl4aMO
m/h
pax2a
I
control
acsl4aMO
ntl

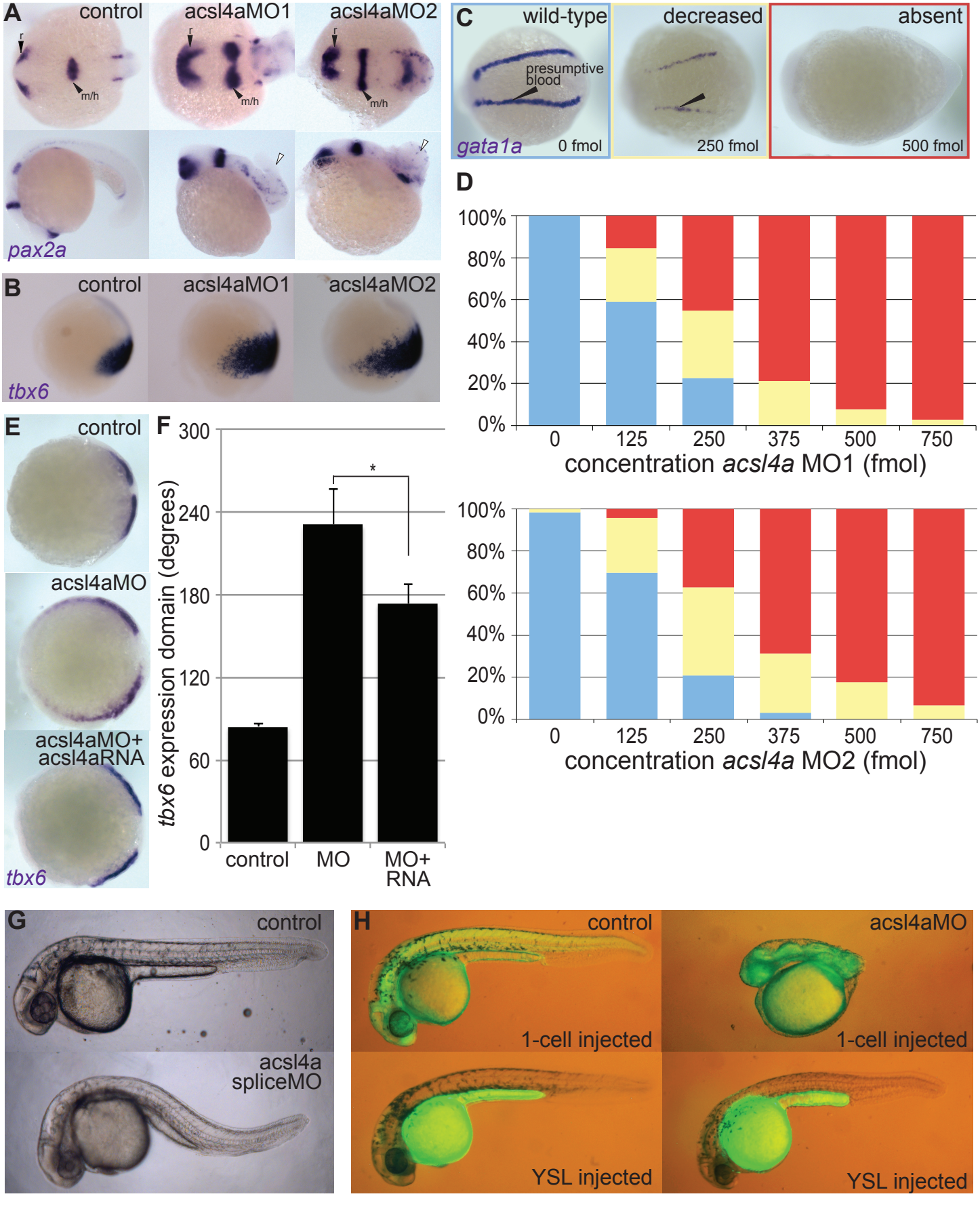
A
control
acsl4aMO1
acsl4aMO2
r
m/h
pax2a
B
control
acsl4aMO1
acsl4aMO2
tbx6
C
wild-type
decreased
absent
presumptive blood
gata1a
0 fmol
250 fmol
500 fmol
D
100%
80%
60%
40%
20%
0%
0
125
250
375
500
750
concentration acsl4a MO1 (fmol)
concentration acsl4a MO2 (fmol)
E
control
acsl4aMO
acsl4aMO+ acsl4aRNA
tbx6
F
tbx6 expression domain (degrees)
300
240
180
120
60
0
*
control
MO
MO+ RNA
G
control
acsl4a spliceMO
H
control
acsl4aMO
1-cell injected
YSL injected

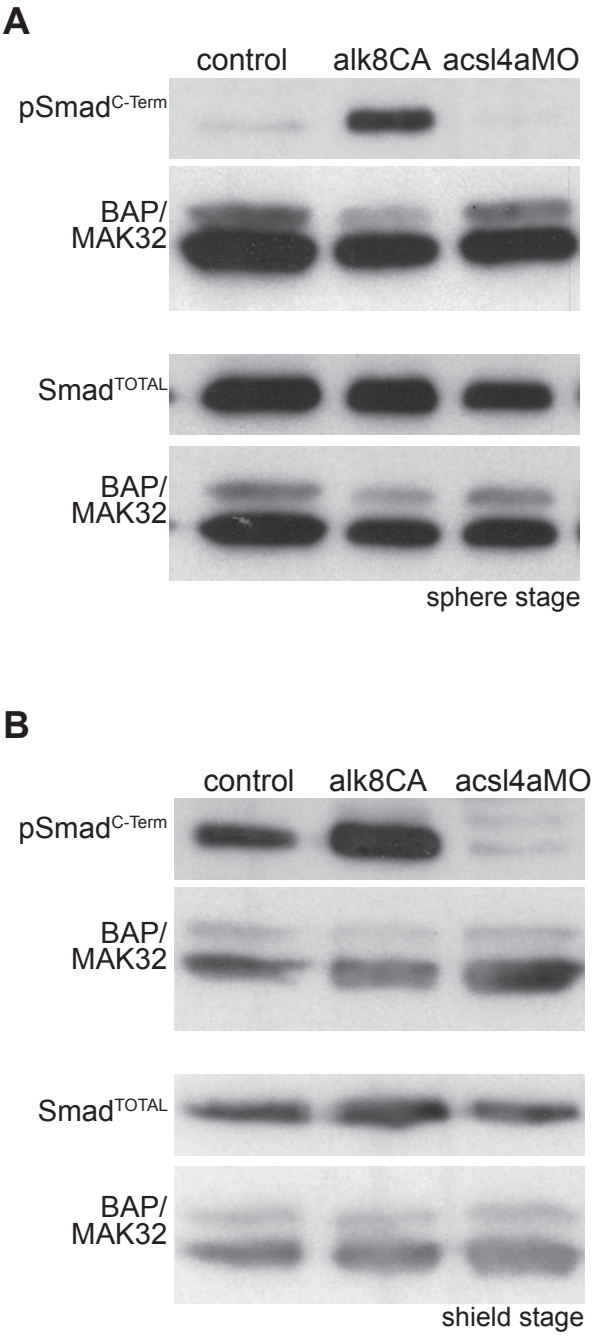
A
control
alk8CA
acsl4aMO
pSmadC-Term
BAP/
MAK32
SmadTOTAL
BAP/
MAK32
sphere stage
B
control
alk8CA
acsl4aMO
pSmadC-Term
BAP/
MAK32
SmadTOTAL
BAP/
MAK32
shield stage

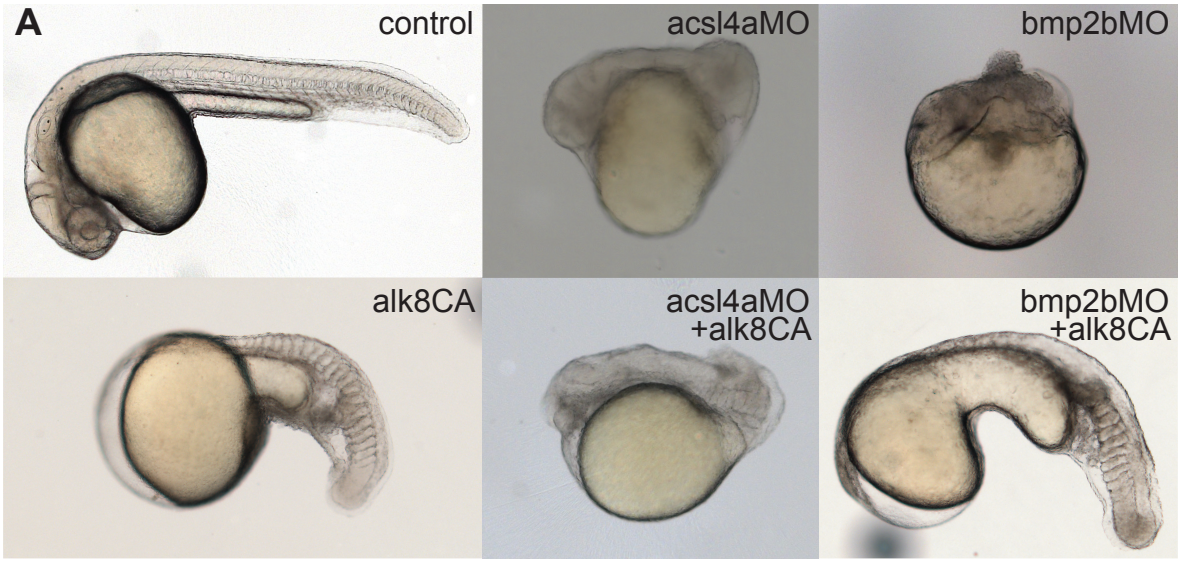
A
control
acsl4aMO
bmp2bMO
alk8CA
acsl4aMO
+alk8CA
bmp2bMO
+alk8CA

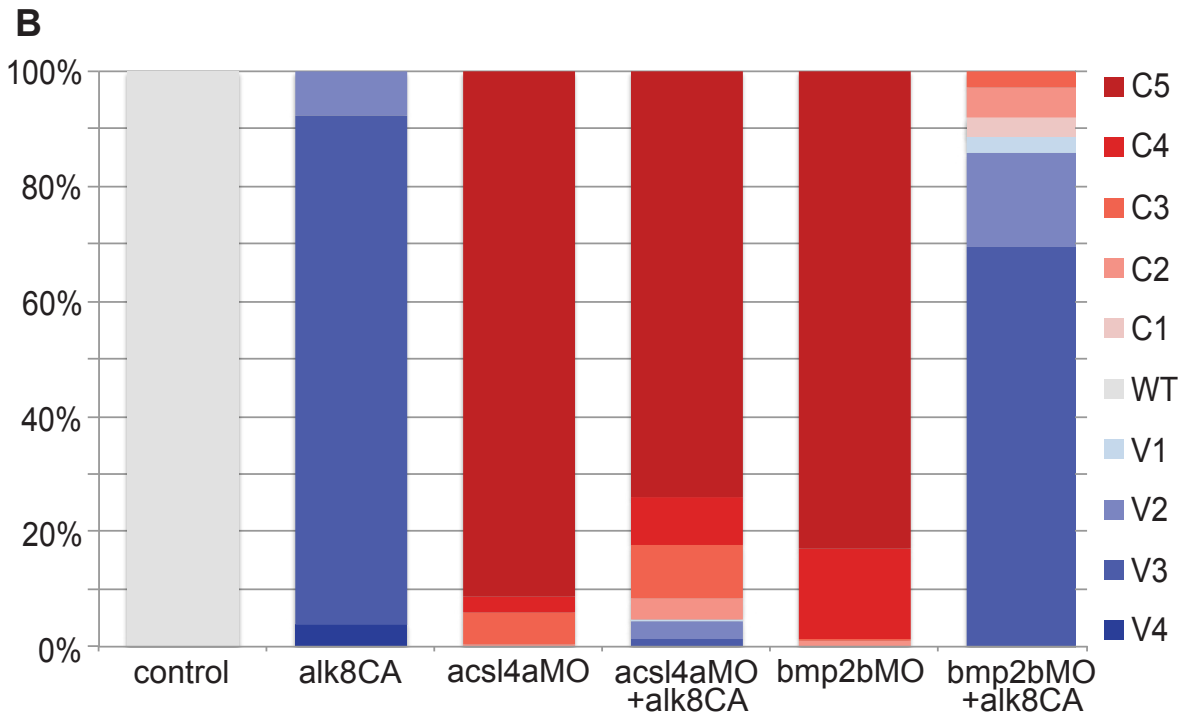
B
100%
80%
60%
40%
20%
0%
control
alk8CA
acsl4aMO
acsl4aMO
+alk8CA
bmp2bMO
bmp2bMO
+alk8CA
C5
C4
C3
C2
C1
WT
V1
V2
V3
V4

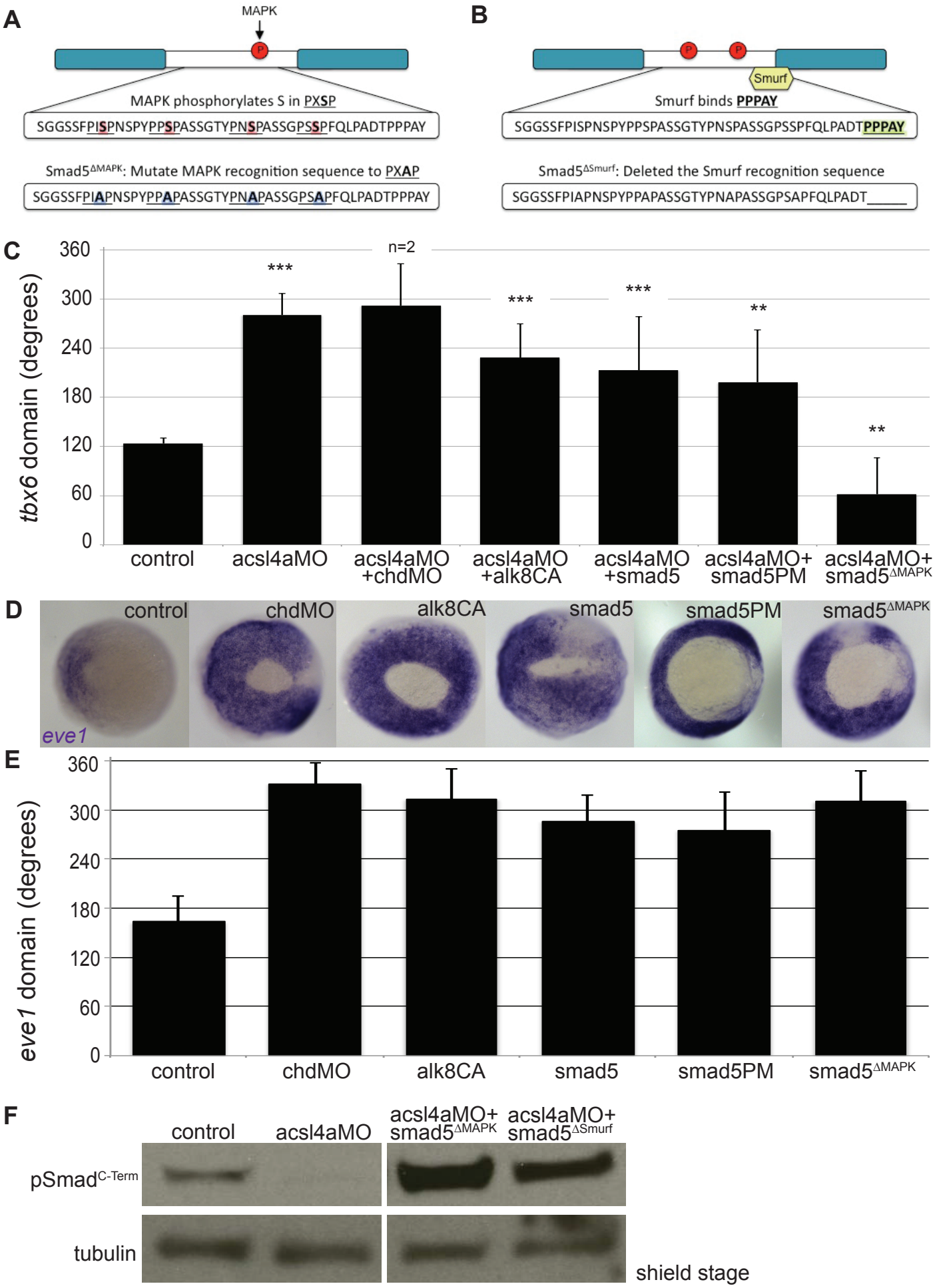
A
MAPK
P
MAPK phosphorylates S in PXSP
SGGSSFPISPNSPYPPSPASSGTYPNSPASSGPSSPFQLPADTPPPAY
Smad5ΔMAPK: Mutate MAPK recognition sequence to PXAP
SGGSSFPIAPNSPYPPAPASSGTYPNAPASSGPSAPFQLPADTPPPAY
B
P
P
Smurf
Smurf binds PPPAY
SGGSSFPISPNSPYPPSPASSGTYPNSPASSGPSSPFQLPADTPPPAY
Smad5ΔSmurf: Deleted the Smurf recognition sequence
SGGSSFPIAPNSPYPPAPASSGTYPNAPASSGPSAPFQLPADT_____
C
tbx6 domain (degrees)
360
300
240
180
120
60
0
n=2
***
***
***
**
**
control
acsl4aMO
acsl4aMO +chdMO
acsl4aMO +alk8CA
acsl4aMO +smad5
acsl4aMO+ smad5PM
acsl4aMO+ smad5ΔMAPK
D
control
chdMO
alk8CA
smad5
smad5PM
smad5ΔMAPK
eve1
E
eve1 domain (degrees)
360
300
240
180
120
60
0
control
chdMO
alk8CA
smad5
smad5PM
smad5ΔMAPK
F
control
acsl4aMO
acsl4aMO+ smad5ΔMAPK
acsl4aMO+ smad5ΔSmurf
pSmadC-Term
tubulin
shield stage

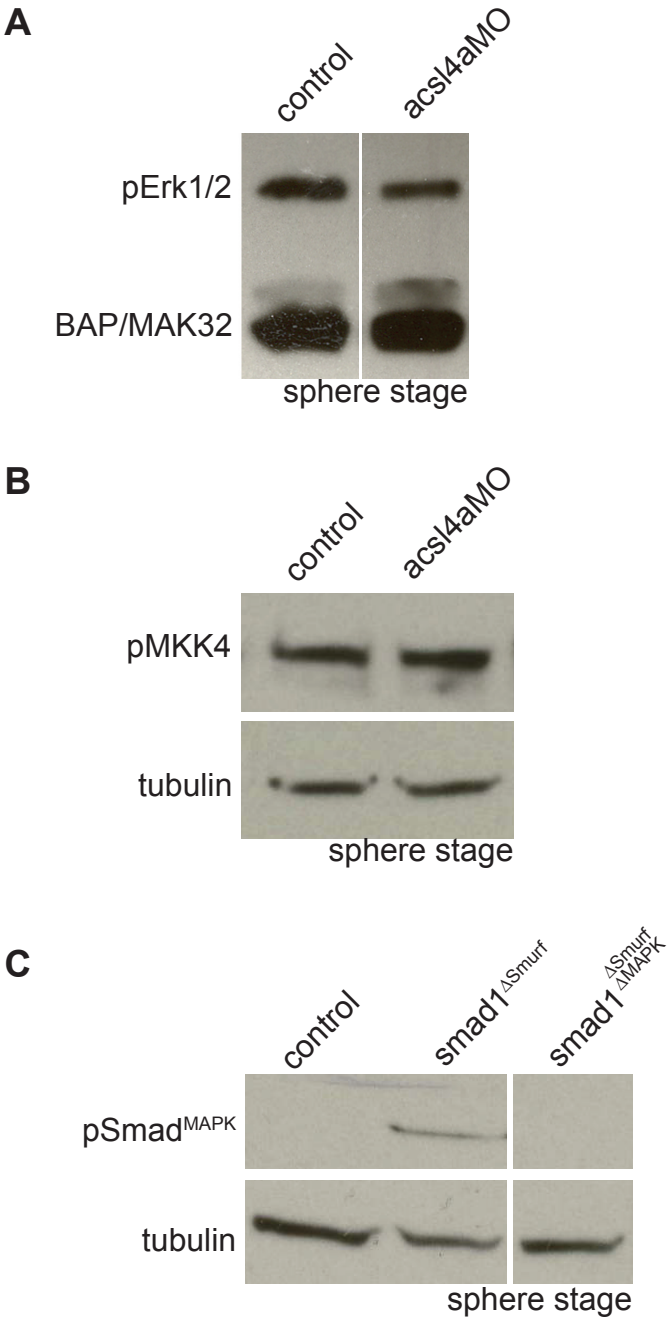
A
control
acsl4aMO
pErk1/2
BAP/MAK32
sphere stage
B
control
acsl4aMO
pMKK4
tubulin
sphere stage
C
control
smad1ΔSmurf
smad1ΔSmurf ΔMAPK
pSmadMAPK
tubulin
sphere stage

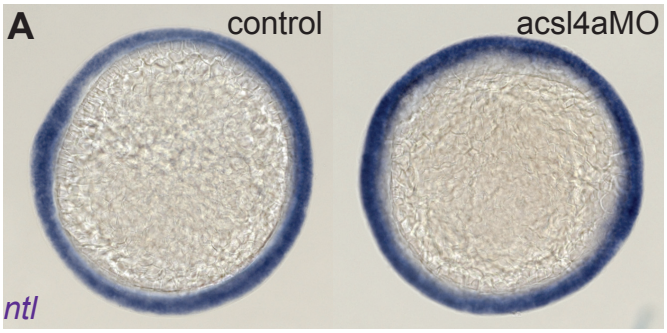

B

MAPK phosphosites:	PX(S/T)P
GSK3 phosphosites:	(S/T)XXX(S_p/T_p)
WW domain binding box:	PPXY
Proline directed phosphosites:	(S/T)P

```
Smad1  180  PNSPTNSYPSSPNSGSGSTATFPHSPSSSDPGSPFQMP-ETPPPAYMPP  234
Smad5  180  PISPNSPYPPSPA-SSG---TYPNSPASSGPSSPFQLPADTPPPAYMPP  231

Smad2  202  GIEPPNNYIPETPPPGYISEDGEASDQQMNQSMDTGSPAELSPSTLSPV  258
Smad3  160  GIEPQSNYIPETPPPGYISEDGETSDHQMNRSMDTGSP-NLSPNPVSPA  215
```

Supplemental Figure Legends

Figure S1: Identification and embryonic expression of zebrafish *acsl4a,* which is necessary for proper dorsoventral patterning, related to Figure 1.

(A-D) Zebrafish Acsl4a is closely related to characterized ACSL4 proteins.

(A) Regions of conserved synteny demonstrate the relationship between human and zebrafish *acsl4* orthologs. Syntenic analysis was performed using reciprocal BLASTN searches of the latest zebrafish (Ensembl Zv9) and human (Ensembl GRCh37) genomic assembly. These data were used to identify the genes adjacent to zebrafish *acsl*4 homologs and search for their human ortholog's chromosomal locations. Genes surrounding both human *ACSL4* and zebrafish *acsl4* genes are shown.

(B) Amino acid sequence comparison of zebrafish (Danio rerio) Acsl4 proteins (*Dr* Acsl4a and *Dr* Acsl4l) to human ACSL4 splice isoforms (*Hs* ACSL4v1 and *Hs* ACSL4v2). Percentages shown are percent identity (ID) and homology (H) determined using BLOSUM62 matrix (Henikoff and Henikoff, 1992).

(C) Motif-II (Black et al., 1992; Kameda and Imai, 1985; Steinberg et al., 2000; Watkins et al., 2007) of ACSL4 homologs. Multiple sequence alignment of ACSL4 orthologs performed using the Jalview software (Clamp et al., 2004; Waterhouse et al., 2009). The MUSCLE algorithm was used with default settings (BLOSUM62). Acsl4l has an amino acid change from Glutamine to Glutamate at position 526 (arrowhead), an amino acid important for arachidonic acid specificity (Stinnett et al., 2007).

(D) Acsl4a contains the homologous N-terminal region of the longer human ACSL4 isoform. Multiple sequence alignment of zebrafish Acsl4 proteins and human ACSL4 splice isoforms performed using the Jalview with MUSCLE. Sequences are colored for percent identity.

(E) *acsl4a* expression in late stage embryonic development. Whole-mount mRNA *in situ* hybridizations using *acsl4a* sense control riboprobe (control) and antisense riboprobe (*acsl4a*). Lateral views, anterior to the left. ysl: yolk syncytial layer, cns: central nervous system.

(F-G) Whole-mount mRNA *in situ* hybridization of *pax2a*/*erg2b*/*myod1* in 12-somite stage embryos either uninjected (control) or injected with 500 fmol *acsl4a* MO. *pax2a* marks m/h: midbrain/hindbrain boundary, o: otic vesicle. *erg2b* marks r3: rhombomere 3, r5: rhombomere 5. *myod1* marks s: somites. (F) Lateral view, anterior to the left. (G) Dorsal view, anterior to the left.

(H) Whole-mount mRNA *in situ* hybridization of *pax2a* in 12-somite stage embryos either uninjected (control) or injected with 500 fmol *acsl4a* MO. Anterior view, dorsal to the right.

(I) Whole-mount mRNA *in situ* hybridization of *ntl* in 12-somite stage embryos either uninjected (control) or injected with 500 fmol *acsl4a* MO. Dorsal view, anterior to the left.

Figure S2: *acsl4a* MOs specifically inhibit maternal *acsl4a* transcripts essential for dorsoventral patterning defect, related to Figure 1.

(A-D) Two translation-blocking *acsl4a* MOs dorsalize zebrafish embryos.

(A) Whole-mount mRNA *in situ* hybridization of *pax2a* in 20 hpf embryos of control, *acsl4a* MO1-injected (750 fmol) or *acsl4a* MO2-injected (750 fmol) embryos. *pax2a* marks m/h: midbrain/hindbrain boundary, r: anterior retina. (top) Dorsal view, anterior to the left. (bottom) Lateral view, anterior to the left. White arrowhead indicates wound-up trunk.

(B) *tbx6*, a marker of dorsal presumptive paraxial mesoderm, is expanded ventrally in *acsl4a* MO1 and *acsl4a* MO2-injected embryos (750 fmol). Lateral view, dorsal to the right.

(C-D) *acsl4a* MOs dose dependently decreases ventral marker *gata1a.*

(C) Representative images of whole-mount mRNA *in situ* hybridization of *gata1a* expression in embryos injected with increasing doses of *acsl4a* MOs. *gata1a* expression was binned into one of three levels: wild-type (blue), decreased (yellow), or absent (red). 8-somite stage embryos. Dorsal view, anterior to the left.

(D) Percentages of embryos with wild-type (blue), decreased (yellow), or absent (red) levels of *gata1a* expression after injection of varying doses of *acsl4a* MOs (*acsl4a* MO1: n=31-50 embryos, from 3 separate experiments; *acsl4a* MO2: n=30-60 embryos, from 3 separate experiments).

(E-F) Injection of *acsl4a* mRNA attenuates the *acsl4a* morphant's dorsalized phenotype.

(E) Representative images of whole-mount mRNA *in situ* hybridization of *tbx6* expression in 80% epiboly stage embryos. Embryos were uninjected (control), injected with *acsl4a* MO1, or injected with *acsl4a* MO1 combined with *acsl4a* mRNA lacking the MO target sequence. Vegetal pole view, dorsal to the right.

(F) Quantification of the angle of *tbx6* expression. Data are mean ± SE of a representative experiment with more than 20 embryos per condition. ANOVA with REGWQ post-hoc test was performed. * $p<0.05$

(G-H) *acsl4a* is required maternally for dorsoventral patterning.

(G) Acsl4a MOs that inhibits splicing of zygotic Acsl4a transcript do not yield dorsoventral patterning defect. Representative bright field images control embryo and embryo injected with *acsl4a* splice-site blocking MO (30 hpf; spliceMO1 1000 fmol).

(H) Acsl4a is not required in the yolk syncytial layer for proper dorsoventral patterning. Representative combined bright-field and fluorescent images of embryos injected with a fluorescein-conjugated MO (control) to indicate injection site or fluorescein-conjugated MO plus *acsl4a* MO (translation blocking acsl4a MO1). 30 hpf, lateral view anterior to the left. (Top) Embryos were injected at the 1-4 cell stage. (Bottom) Embryos were injected into the yolk syncytial layer (YSL) at 1K-cell stage. The MOs were restricted from the cells of the embryo proper. 99% of embryos injected at the 1-cell stage with acsl4a MO were dorsalized in comparison to 3% of those injected in the YSL (n=92-93 embryos from 4 experiments). Embryos injected with control MO into the YSL also had

occasional dorsalization (4%, n=52 embryos from 3 experiments), whereas 0% of control embryos injected at the 1-cell stage were dorsalized.

Figure S3: Bmp signaling is dependent on Acsl4a, related to Figure 2.

Representative western blots of C-Terminal phosphorylated (pSmad$^{C\text{-}Term}$) and pan Smad1/5/8 (Smad^{Total}) from control embryos and embryos injected with *alk8CA* mRNA (20-40 pg), *acsl4a* MO (500 fmol). Anti-BAP/MAK32 is shown as a loading control.

(A) Lysates from sphere-stage embryos.

(B) Lysates from shield-stage embryos.

Figure S4: Acsl4a is epistatic to the Bmp receptor Alk8, related to Figure 3.

(A) Representative bright-field images of 24 hpf embryos injected with 500 fmol *acsl4a* MO (class C4), 50 fmol *bmp2b* MO (class C5), 20-40 pg constitutively active (CA) *alk8* mRNA (class V3), a combination of *acsl4a* MO and *alk8CA* mRNA (class C4), or a combination of *bmp2b* MO and *alk8CA* mRNA (class V3). Lateral view, anterior to the left.

(B) Percentages of phenotypic classes. Dorsalization: strong (C5) to weak (C1). Ventralization: strong (V4) to weak (V1). n=283-298 embryos, from 3 separate experiments.

Figure S5: Epistasis analysis of Bmp signaling cascade, related to Figure 4.

(A-B) Diagrams of Smad5 constructs, showing mutated residues in the linker region.

(A) MAPK-insensitive Smad5: Smad5$^{\Delta MAPK}$

(B) Non degradable Smad5: Smad5$^{\Delta Smurf}$

(C) Quantification of the angle of *tbx6* expression from whole-mount *in situ* hybridization after injection with acsl4a MO (750 fmol) alone or combined with *chordin* morpholino (chdMO 20fmol), constitutively active *alk8* mRNA (alk8CA 1.5 ng) mRNA, C-terminal phosphomimic s*mad5* (smad5PM 1.5 ng) mRNA, and MAPK-insensitive *smad5* (smad5$^{\Delta MAPK}$ 1.5 ng) mRNA. Data are represented as mean of experimental means ± pooled SE. For *acsl4a* MO+ *chordin* MO, data are represented as mean of experimental means ± pooled SD (n=2-8 experiments, 12-80 embryos/experiment). ANOVA with Dunnett post-hoc test was performed; *acsl4a* MO+ *chordin* MO data was excluded from analysis. ** $p \leq 0.005$, *** $p < 0.0001$: compared to control.

(D-E) Constructs used for rescue analysis in Figures 2B&C, 4B&C and S5A ventralize embryos to a similar extent.

(D) Whole-mount *in situ* hybridization of ventral mesoderm marker *eve1* after injection with chdMO or mRNAs from Figures 2B&C, 4B&C and S5A. Injections were performed in parallel (i.e., with the same injection needle) with those in Figures 2B&C, 4B&C and S5A. Vegetal pole view, dorsal to the right (80% epiboly).

(E) Data are represented as mean of experimental means ± pooled SD (n=2-7 experiments, 8-47 embryos/experiment).

(F) Smad5 mutant constructs are phosphorylated by the Bmp receptor independent of Acsl4a. Representative western blot (n=4) of C-Terminal phosphorylated Smad ($pSmad^{C\text{-}Term}$) from control embryos, embryos injected with *acsl4a* MO (750 fmol) or embryo injected with acsl4a MO combined with $smad5^{\Delta MAPK}$ (1.5 ng) or $smad5^{\Delta Smurf}$ (1.5 ng) mRNA. Anti-alpha tubulin is shown as a loading control. An extraneous lane between *acsl4a* MO and *acsl4a* MO+ $smad5^{\Delta MAPK}$ is omitted.

Figure S6: Acsl4a does not activate Erk1/2 or Jnk MAPK cascades, related to Figure 5.

(A) Erk1/2 is not activated in *acsl4a* morphants. Representative western blot of phosphorylated Erk1/2 from control embryos and embryos injected with *acsl4a* MO (500 fmol) at sphere stage. Anti-BAP/MAK32 is shown as a loading control. An extraneous lane is omitted. pERK1/2 levels in acsl4a MO-injected embryos are 90±19% of control (not significant, n=3).

(B) Jnk signaling cascade is not activated in *acsl4a* morphants. Representative western blot of phosphorylated MKK4 from control embryos and embryos injected with *acsl4a* MO (750 fmol) at sphere stage. Blots were stripped and probed with alpha tubulin as a loading control. pMKK4 levels in acsl4a MO-injected embryos are 1.57 ± .82% of control (not significant, n=4).

(C) Representative western blot (n=3) testing the antibody against MAPK phosphorylated hSmad1 (pSmad$^{\Delta MAPK}$) (gift of Eddie de Robertis (Fuentealba et al., 2007)) on zebrafish Smad constructs (1 ng). An extraneous lane between *smad1*$^{\Delta Smurf}$ and *smad1*$^{\Delta Smurf\Delta MAPK}$ is omitted.

Figure S7: Acsl4a does not significantly alter Smad2/3 signaling, related to Figure 7.

(A) Whole-mount mRNA *in situ* hybridization of *ntl* in 50% epiboly stage embryos, uninjected (control) or injected with 500 fmol *acsl4a* MO. Animal pole view. 96% of acsl4a MO-injected embryos appear wild-type (n=3 experiments; 127 embryos). (B) Sequence alignment of zebrafish Smad1/5 and Smad2/3 linker regions with important residues highlighted.

Supplemental Experimental Procedures

Syntenic Analysis

Regions of shared or conserved synteny were determined by exploring the latest genomic assemblies of zebrafish (Ensembl Zv9) and human (Ensembl GRCh37). Syntenic analysis was performed by reciprocal BLASTN searches of the genes immediately surrounding the zebrafish *acsl* genes to look for the human ortholog. Only orthologous genes were shown.

mRNA synthesis, cloning and mutagenesis

Full-length *acsl4a* coding sequence was PCR amplified from zebrafish cDNA with iProof polymerase (Bio-Rad Labs). An ideal Kozak sequence (GCCACC) was added. The resulting amplicon was cloned into a pCS2+ based gateway destination vector, pCSDest (gift of Lawson Lab). The following primers were used for cloning *acsl4a* for mRNA synthesis:

Forward: GCCACC**ATG**GACCTCAGTGCCGTTC

Reverse: **CTA**CTTGTGGCCATACATTCTTTC

AKT-1/PKBα (Ramaswamy et al., 1999)Addgene #9005) was cloned into pCS2+. The following mutated versions of pCSDest-Acsl4a, p64TS-Smad5 (Hild et al., 1999) and pCS2^{+}-Smad1 (Dick et al., 1999) were created by site-directed mutagenesis (Stratagene):

Acsl4aCI (G437L), Smad5PM (S461D/S462D/S464D), Smad5$^{\Delta MAPK}$ (S189A/S197A/S207A/S215A), Smad5$^{\Delta Smurf}$ (Δ224-228), Smad5$^{\Delta MAPK\Delta Smurf}$

(S189A/S197A/ S207A/S215A, Δ224-228), Smad1$^{\Delta MAPK}$ (S189A/S197A/S211A/ S219A), Smad1$^{\Delta Smurf}$ (Δ227-231), and Smad1$^{\Delta MAPK\Delta Smurf}$ (S189A/S197A/S211A/ S219A, Δ227-231).

Morpholinos

The two MOs targeting Acsl4a 5'UTR are:

MO1: TCTGCTGAGAAGCTGGAGGGGACTG and

MO2: GGACTGAAGGATGAAGGGTCAGGCA.

The MOs targeting Acsl4a splice junctions are:

Splice1: GGTTTCTTAAATAAAAGCTCACCTT (Figure S3A),

Splice2: AGCTCACCTTTAGTTTTGTTTCCAG, and

Splice3: GAAGAAGAACACTCTACATGGGAAT.

chordin MO: ATCCACAGCAGCCCCTCCATCATCC (Nasevicius and Ekker, 2000), *bmp2b* MO: CGCGGACCACGGCGACCATGATC (Lele et al., 2001) and FITC MO: fluorescein-tagged CTTTCCAGGTCCCGTTGAAGGTCAT were also used.

Microinjection of zebrafish embryos

For mRNA and MOs, injection solutions were made in H_2O or Danieau buffer containing 0.2% phenol red. A volume of 1-3 nl was injected into embryos with a microforged glass needle connected to a N_2 gas pressure injector (P420 picopump, World Precision Instruments) or (PL1–100, Harvard Apparatus). For most experiments, embryos were injected from the 1-4 cell stage. For YSL

injections, embryos were injected at the 1000-cell to high-stage (3-3.5 hpf) into the newly formed YSL.

in situ probes

Trizol-prepared zebrafish total RNA was oligo-dT primed and AMV Reverse transcriptase amplified to synthesize cDNA for PCR cloning. For *in situ* probes against *acsl4a, pax2a, erg2b, ntl* and *gata1a*, 500+ base pairs of transcript-specific sequence were amplified from cDNA. All primers were designed to amplify a region spanning an intron. Amplicons were TA cloned into the dual promoter pCRII-TOPO® vector (Invitrogen) for both sense and antisense probe synthesis. *In situ* probes were synthesized using the DIG RNA labeling kit and SP6 or T7 polymerase (Roche), according to the manufacturer's instruction.

In situ hybridization was performed using the following published probes: *bmp2b* (Martinez-Barbera et al., 1997), *bmp7a* (Hild et al., 1999), *tbx6* (Nikaido et al., 2002), *eve1* (Joly et al., 1993), *foxb1.2* (Furutani-Seiki et al., 1996), *gata1a* (Detrich et al., 1995), *myod1* (Weinberg et al., 1996), *pax2a* (Krauss et al., 1991), *egr2b* (Oxtoby and Jowett, 1993), *ntl* (Schulte-Merker et al., 1994) and *gata2a* (Detrich et al., 1995).

Whole-mount immunohistochemistry

For Figure 2D, anti-phosphoSmad1/5/8 antibody (Cell Signaling Technology) and a biotinylated goat anti-rabbit secondary antibody (Jackson ImmunoResearch

Labs) were used at a concentration of 1:200 and detection was performed using the Vectastain ABC Kit (Vector Laboratories). For Figure 2E, fluorescein was detected with anti-fluorescein/Oregon Green AlexaFluor488 (Invitrogen) and pSmad1/5$^{C\text{-}Term}$ was detected with anti-phosohoSmad1/5/8 (Cell Signaling Technology) and AlexaFluor647 goat anti-rabbit (Invitrogen), each at 1:200.

pSmad$^{C\text{-}Term}$ Signal Quantification

A subset of transplanted cells was quantified for pSmad$^{C\text{-}Term}$ signal intensities (data represent transplanted cells into 5-6 embryos/group from 2-3 experiments). Relative fluorescence signal intensities of nuclear pSmad$^{C\text{-}Term}$ staining were determined for individual cells and normalized to DAPI intensities of the same cells. Quantification of fluorescence signals was determined using ImageJ.

Western Blot

Western Blots were performed slightly differently in the two labs.

<u>For blots in Figures 3, 6, S3, and S6A:</u>

Manually dechorionated embryos were dissociated in Ca^{2+}-free Ringer's solution. Cells were separated from yolk (and debris) by centrifugation. Protein extracts were prepared by standard procedures (Sambrook and Russell, 2001) and separated on 9% or 12% polyacrylamide gels (~13 embryos/lane). Protein extracts concentrations were determined using the DC Protein Assay kit (Bio-

Rad Labs). Proteins were transferred on to Nitrocellulose membranes and Ponceau S staining was used to ensure proper transfer. Membranes were blocked with 4% BSA/TBST. Jackson ImmunoResearch Labs' secondary antibodies were used. ECL Western Blotting detection reagent (Pierce) was used for detection.

For blots in Figures 2, 5, and S6B&C:

Staged embryos were either snap frozen (manually dechorionated) or fixed in 100% ice-cold acetone overnight. Fixed embryos were rehydrated in PBS and manually dechorionated. For embryos 30% epiboly and younger, the yolk was manually removed with forceps. Protein extracts were prepared by standard procedures (Sambrook and Russell, 2001) and separated on 8.5% or 10% polyacrylamide gels (3-10 embryos/lane). Proteins were transferred on to PVDF membranes (Millipore). Ponceau S staining was used to ensure proper transfer. Membranes were blocked with 5% skim milk in TBST. Biorad secondary antibodies were used. The anti-Rabbit secondary antibody and pSmad^{MAPK} primary antibody were preabsorbed on membranes that had only yolk proteins (from the manually removed yolks described above). To probe with additional antibodies, membranes were stripped with Restore^{TM} stripping reagent (Pierce) according to manufacturer's instruction. Supersignal West Pico or Femto Western Blotting detection reagent (Pierce) was used for detection.

Primary Antibodies for Western Blot

	Antibody Target	Source	Concentration
pSmad$^{C\text{-}Term}$	Phospho-Smad1 (Ser463/465)/ Smad5 (Ser463/465)/ Smad8 (Ser426/428)	Cell signaling Technology	1:1,000
Smad^{Total}	Smad1/5/8 (N-18)	Santa Cruz	1:1,000
pSmad^{MAPK}	Phospho-human Smad1 (Ser214)	gift from Eddie de Robertis (Fuentealba et al., 2007)	1:1,000
p38^{Active}	Phospho-p38 (Thr180/Tyr182)	Cell signaling Technology	1:1,000
MKK4^{Active}	Phospho-SEK1/MKK4 (Ser257/Thr261)	Cell signaling Technology	1:1,000
Erk1/2^{Active}	Activated (Diphosphorylated) ERK-1&2	Sigma-Aldrich	1:1,000
GSK3^{Total}	GSK-3β	Cell signaling Technology	1:1,000
GSK^{Inactive}	Phospho-GSK-3α/β (Ser21/9)	Cell signaling Technology	1:1,000
Tubulin	Alpha-tubulin	Sigma-Aldrich	1:10,000
BAP/MAK32	BAP32/MAK32	gift from W.W. Schamel (Adachi et al., 1996).	1:3,000

Secondary Antibodies for Western Blot

Secondary Antibody	Source	Concentration
anti-rabbit HRP	Jackson ImmunoResearch	1:5,000
anti-mouse HRP	Jackson ImmunoResearch	1:5,000
anti-rabbit HRP	Biorad	1:10-1:20K
anti-mouse HRP	Biorad	1:40K

Western Blot quantification

Film and optical density standards were scanned in the transmissive mode of desktop scanners. Using optical density standards, scans were either converted to scaled optical density (Matlab) or were calibrated using the Rodbard curve fitting function of ImageJ. ImageJ was used to determine the band intensities. Experimental data was normalized to either BAP/MAK32 or Tubulin loading controls.

RNA-seq

AB embryos were injected (1-4 cell) with 2 nl of either: (1) 500 fmol of Acsl4a MO1 plus 250 fmol of fluoresceinated control MO (FITC MO, see above) and 0.2% phenol red or (2) 250 fmol of FITC MO and phenol red 0.2%. The FITC MO was used as a control to determine that each embryo was properly injected; embryos were confirmed for fluorescein fluorescence and examined for healthy appearance. Embryos (20 embryos/tube) were processed at 80% epiboly. A fraction of the embryos (10-20) were raised to ~20 somites to confirm the morphant phenotype as well as health of control group.

Total RNA was prepared with Trizol according to the manufacturer's instructions, genomic DNA was digested with RNase free DNase, and the RNA was purified with RNeasy Plus Mini Kit (Qiagen). RNA samples were sent to the Johns Hopkins Deep Sequencing & Microarray Core Facility where staff constructed a mRNA library for RNA-seq, performed the sequencing and analyzed the resulting data.

Supplemental References:

Adachi, T., Schamel, W.W., Kim, K.M., Watanabe, T., Becker, B., Nielsen, P.J., and Reth, M. (1996). The specificity of association of the IgD molecule with the accessory proteins BAP31/BAP29 lies in the IgD transmembrane sequence. EMBO J *15*, 1534-1541.

Black, P.N., DiRusso, C.C., Metzger, A.K., and Heimert, T.L. (1992). Cloning, sequencing, and expression of the fadD gene of Escherichia coli encoding acyl coenzyme A synthetase. The Journal of biological chemistry *267*, 25513-25520.

Clamp, M., Cuff, J., Searle, S.M., and Barton, G.J. (2004). The Jalview Java alignment editor. Bioinformatics *20*, 426-427.

Detrich, H.W., 3rd, Kieran, M.W., Chan, F.Y., Barone, L.M., Yee, K., Rundstadler, J.A., Pratt, S., Ransom, D., and Zon, L.I. (1995). Intraembryonic hematopoietic cell migration during vertebrate development. Proc Natl Acad Sci U S A *92*, 10713-10717.

Dick, A., Meier, A., and Hammerschmidt, M. (1999). Smad1 and Smad5 have distinct roles during dorsoventral patterning of the zebrafish embryo. Dev Dyn *216*, 285-298.

Fuentealba, L., Eivers, E., Ikeda, A., Hurtado, C., Kuroda, H., Pera, E.M., and De Robertis, E.M. (2007). Integrating patterning signals: Wnt/GSK3 regulates the duration of the BMP/Smad1 signal. Cell *131*, 980-993.

Furutani-Seiki, M., Jiang, Y.J., Brand, M., Heisenberg, C.P., Houart, C., Beuchle, D., van Eeden, F.J., Granato, M., Haffter, P., Hammerschmidt, M.*, et al.* (1996).

Neural degeneration mutants in the zebrafish, Danio rerio. Development *123*, 229-239.

Henikoff, S., and Henikoff, J.G. (1992). Amino acid substitution matrices from protein blocks. Proc Natl Acad Sci U S A *89*, 10915-10919.

Hild, M., Dick, A., Rauch, G.J., Meier, A., Bouwmeester, T., Haffter, P., and Hammerschmidt, M. (1999). The smad5 mutation somitabun blocks Bmp2b signaling during early dorsoventral patterning of the zebrafish embryo. Development *126*, 2149-2159.

Joly, J.S., Joly, C., Schulte-Merker, S., Boulekbache, H., and Condamine, H. (1993). The ventral and posterior expression of the zebrafish homeobox gene eve1 is perturbed in dorsalized and mutant embryos. Development *119*, 1261-1275.

Kameda, K., and Imai, Y. (1985). Isolation and characterization of the multiple charge isoforms of acyl-CoA synthetase from Escherichia coli. Biochimica et biophysica acta *832*, 343-350.

Krauss, S., Johansen, T., Korzh, V., and Fjose, A. (1991). Expression of the zebrafish paired box gene pax[zf-b] during early neurogenesis. Development *113*, 1193-1206.

Lele, Z., Bakkers, J., and Hammerschmidt, M. (2001). Morpholino phenocopies of the swirl, snailhouse, somitabun, minifin, silberblick, and pipetail mutations. Genesis *30*, 190-194.

Martinez-Barbera, J.P., Toresson, H., Da Rocha, S., and Krauss, S. (1997). Cloning and expression of three members of the zebrafish Bmp family: Bmp2a, Bmp2b and Bmp4. Gene *198*, 53-59.

Nasevicius, A., and Ekker, S.C. (2000). Effective targeted gene 'knockdown' in zebrafish. Nat Genet *26*, 216-220.

Nikaido, M., Kawakami, A., Sawada, A., Furutani-Seiki, M., Takeda, H., and Araki, K. (2002). Tbx24, encoding a T-box protein, is mutated in the zebrafish somite-segmentation mutant fused somites. Nature genetics *31*, 195-199.

Oxtoby, E., and Jowett, T. (1993). Cloning of the zebrafish krox-20 gene (krx-20) and its expression during hindbrain development. Nucleic Acids Res *21*, 1087-1095.

Ramaswamy, S., Nakamura, N., Vazquez, F., Batt, D.B., Perera, S., Roberts, T.M., and Sellers, W.R. (1999). Regulation of G1 progression by the PTEN tumor suppressor protein is linked to inhibition of the phosphatidylinositol 3-kinase/Akt pathway. Proc Natl Acad Sci U S A *96*, 2110-2115.

Sambrook, J., and Russell, D.W. (2001). Molecular cloning : a laboratory manual, 3rd edn (Cold Spring Harbor, N.Y., Cold Spring Harbor Laboratory Press).

Schulte-Merker, S., van Eeden, F.J., Halpern, M.E., Kimmel, C.B., and Nusslein-Volhard, C. (1994). no tail (ntl) is the zebrafish homologue of the mouse T (Brachyury) gene. Development *120*, 1009-1015.

Steinberg, S.J., Morgenthaler, J., Heinzer, A.K., Smith, K.D., and Watkins, P.A. (2000). Very long-chain acyl-CoA synthetases. Human "bubblegum" represents a

new family of proteins capable of activating very long-chain fatty acids. The Journal of biological chemistry *275*, 35162-35169.

Stinnett, L., Lewin, T.M., and Coleman, R.A. (2007). Mutagenesis of rat acyl-CoA synthetase 4 indicates amino acids that contribute to fatty acid binding. Biochim Biophys Acta *1771*, 119-125.

Waterhouse, A.M., Procter, J.B., Martin, D.M., Clamp, M., and Barton, G.J. (2009). Jalview Version 2--a multiple sequence alignment editor and analysis workbench. Bioinformatics *25*, 1189-1191.

Watkins, P.A., Maiguel, D., Jia, Z., and Pevsner, J. (2007). Evidence for 26 distinct acyl-coenzyme A synthetase genes in the human genome. Journal of lipid research *48*, 2736-2750.

Weinberg, E.S., Allende, M.L., Kelly, C.S., Abdelhamid, A., Murakami, T., Andermann, P., Doerre, O.G., Grunwald, D.J., and Riggleman, B. (1996). Developmental regulation of zebrafish MyoD in wild-type, no tail and spadetail embryos. Development *122*, 271-280.